OPEN ACCESS

IOP Publishing

Superconductor Science and Technology

Supercond. Sci. Technol. **33** (2020) 015003 (9pp)

https://doi.org/10.1088/1361-6668/ab5b46

Characterisation of the mechanical failure and fracture mechanisms of single grain Y–Ba–Cu–O bulk superconductors

Jasmin V J Congreve[1], Yunhua Shi, Kai Yuan Huang, Anthony R Dennis, John H Durrell and David A Cardwell

Department of Engineering, University of Cambridge CB2 1PZ, Cambridge, United Kingdom

E-mail: jvjc2@cam.ac.uk

Received 1 October 2019, revised 7 November 2019
Accepted for publication 25 November 2019
Published 11 December 2019

Abstract

The widespread use of melt processed, single grain (RE)–Ba–Cu–O bulk superconductors [(RE)BCO], where RE = Y, Gd or Sm, is limited predominantly by the poor mechanical properties of these inherently brittle, ceramic-like materials. The high density of flaws, such as cracks and voids, within the single grain microstructure leads directly to a low fracture toughness. As a result, the Lorentz forces, generated when these materials carry current in the presence of a large magnetic field, create stresses sufficiently large to cause brittle failure. The addition of Ba–Cu–O (liquid phase) and Ag to the precursor composition prior to melt-growth has been demonstrated to be effective in improving the mechanical properties of these technologically important materials. In this work, we characterise the mechanical failure of single grain YBCO bulk superconductors in terms of a Weibull statistical distribution. In addition, differences in fracture mechanisms have been studied to provide a better understanding of how the provision of additional liquid phase and silver produces YBCO single grains with better resulting mechanical properties and how these can be improved further.

Keywords: YBCO, YBCO-Ag, mechanical properties, failure

(Some figures may appear in colour only in the online journal)

Introduction

Single grain (RE)$Ba_2Cu_3O_{7-\delta}$ [(RE)-123] bulk high temperature superconductors (HTS), where RE is a rare earth element such as Y, Gd or Sm, are able to trap magnetic fields that are significantly larger than those generated by conventional, Fe-based permanent magnets, leading to potential for the development of a wide range of practical applications [1–3]. However, during magnetisation and operation at high fields, large stresses are generated within the microstructure of the bulk sample due to the interaction of transport current and flux vortex lines. As a result, the brittle nature of these materials limits severely the exploitation of their superconducting properties for applications that require relatively high magnetic fields [4, 5].

Despite the limits imposed by mechanical considerations on the exploitation of superconducting properties, relatively limited research has been performed on the mechanical properties [6–8] and fracture mechanisms [9, 10] of these materials. A number of studies have measured the fracture toughness of various (RE)BCO systems using indentation testing [9–12] or by carrying out tensile tests on V-notched specimens cut from bulk, single grain superconductors [13]. These studies reveal that their fracture toughness is both anisotropic and low in comparison to engineering ceramics such as SiC and Al_2O_3 [9], which is likely to be due to the high level of porosity present typically in YBCO bulk single grains. It has been observed that the addition of secondary phase particles, such as $(RE)_2BaCuO_5$ (RE-211) inclusions

[1] Author to whom any correspondence should be addressed.

trapped within the continuous RE-123 phase matrix, enhance the fracture toughness [12, 14, 15], since they tend to resist and deflect crack propagation [12, 15]. In addition, the flexural strength of beams of YBCO [7, 8, 13, 16, 17], YBCO-Ag [8] and GdBCO-Ag [7] cut from parent single grain bulk superconductors have been analysed previously. The flexural strength of a small number of YBCO-Ag beams have also been tested at 77 K [18]. More recent work has investigated the strength of a number of whole YBCO [7, 17] and GdBCO-Ag [7] bulk superconductors using the so-called 'Brazilian test', which uses an indirect approach to effectively sample a larger specimen volume [19]. The failure surfaces of a number of SmBCO-Ag specimens have also been studied [20]. However, more detailed and comprehensive studies of the mechanisms of failure and the fracture behaviour of (RE)BCO samples is required to provide important insight into how these materials fail and hence to develop effective techniques to prevent or reduce the likelihood of failure, particularly in practical applications.

Several inter-dependent, and often conflicting, factors need to be considered carefully to obtain bulk superconductors that exhibit high values of J_c. A large single grain sample free of high-angle grain boundaries is required for practical devices [21–23]. The presence of poorly connected grain boundaries in (RE)BCO superconductors reduces significantly the flow of supercurrent within the bulk sample, which, in turn, reduces the size of the current loops and therefore the magnitude of the trapped field generated by the sample [24, 25]. In addition, these materials must have a uniform distribution of flux pinning inclusions, such as Y-211, in order to achieve good superconducting properties [25–27]. Alongside this, these materials require good mechanical properties to enable their effectiveness in applications, and especially those requiring high magnetic fields [28].

The introduction of silver into YBCO bulk single grains has been shown to improve significantly the mechanical properties of this material [8] and single grain bulk materials of YBCO-Ag can now be grown successfully by a number of groups [29]. More critically, the addition of silver to this material does not have a detrimental effect on its superconducting properties and is therefore a viable solution to improving the mechanical properties of this system [30].

Initial research into the mechanical properties of YBCO-Ag focused on simple comparisons of the results of three-point bend tests [8]. However, the maximum strength often varies from sample to sample due to the brittle nature of these materials, even for samples of identical size and tested nominally under the same experimental conditions. This is because the failure of a ceramic depends on the flaws present within the microstructure, with cracks initiated predominantly at regions of weakness, such as internal pores. The failure of a ceramic sample occurs at the most critical flaw present within its microstructure, which is often referred to as the weakest link (typically the longest crack present) [31]. As the size and distribution of flaws vary throughout each bulk sample, the strength of these materials can be best represented as a distribution related to the probability of failure. The Weibull distribution is used for this purpose [17, 32, 33]. There are two parameters used to define this distribution; *m,* the Weibull modulus, which relates to the homogeneity of the flaws present and σ_o, which describes the level of force required to break 63.5% of the samples tested. 'Poor' ceramics generally exhibit a low level of homogeneity and are characterised by a value of m roughly between 0 and 10, whereas 'tough' ceramics show significantly more homogeneity and typically exhibit $m > 10$. The Weibull distribution is given by:

$$P_f = 1 - e^{-\left[\frac{\sigma}{\sigma_0}\right]^m}, \quad (1)$$

where P_f is the probability of failure, σ is the stress, σ_0 is the stress at which 63.5% of the samples fail and m is the Weibull modulus, which is an indirect measure of the homogeneity of flaws present [33].

The majority of engineering ceramics are compacted and sintered and so contain a completely random distribution of flaws. As a result, the critical flaw that leads to failure could occur anywhere within the sample microstructure. In contrast, however, porosity and cracking varies significantly between different regions of the sample in (RE)BCO single grain superconductors. Consequently, in these samples, the average pore size usually correlates with location. Although there is usually a predictable average pore size at a given location, there is still a large degree of variation within the sample microstructure, and a large pore or crack could be present at any point. Given that failure is governed by the most critical flaw present and this could occur at any location, the Weibull modulus remains a good model to evaluate the strength of YBCO bulk superconductors. In addition, due to the nature of the melt-growth process, there are often differences in the microstructures and properties of single grains of a given sample type grown under the same conditions. Therefore, it is critical to study a number of these single grains in a meaningful investigation of mechanical stability.

In this work the trapped field was measured to ensure comparable superconducting properties were achieved in the YBCO-Ag and YBCO samples. The Weibull distribution for single grain YBCO and YBCO-Ag samples fabricated by top seeded melt-growth (TSMG) and for single grain YBCO fabricated by liquid phase enriched TSMG has been derived subsequently from a detailed study of a large quantity of 3-point bend test data. In total, 162 failure surfaces have been examined in order to deduce how to reduce the likelihood of failure and increase the flexural strength of single grain, YBCO bulk superconductors.

Method

Sample growth

Three samples of YBCO were prepared by conventional TSMG [34]. These samples were pressed uniaxially in a 30 mm diameter cylindrical die from 99.9% purity powders of Y-123:Y-211:CeO_2 in the mass ratio 150:50:1. Three further samples were grown by liquid-phase-enriched TSMG [34], and labelled LR YBCO. Precursor powder was mixed in the same ratio as for standard YBCO and an additional 4.6 g

powder layer mixed from Yb_2O_3:$Ba_3Cu_5O_8$:BaO_2 in the ratio 5.0:5.6:1.0, which had been calcined once for 5 h at 850 °C, was compacted in the die below the precursor powder. Finally, three samples of YBCO-Ag were grown by liquid-phase-enriched TSMG [35]. Precursor powder was mixed from 99.9% purity powders of Y-123:Y-211:CeO_2:Ag_2O in a mass ratio of 150:50:1:20 and liquid-phase-rich powder was mixed and calcined as described above. Composite green pellets were pressed with a 4.6 g layer of liquid-phase powder below 46 g of precursor powder.

After melt processing, all 9 samples were annealed in oxygen for 8 d at 450 °C in order to transform the Y-123 tetragonal structure to the superconducting orthorhombic structure.

Measurement of trapped field

The top and base of each of the nine samples was polished flat and parallel using grade 180 grit silicon carbide paper. The maximum trapped field at the top and bottom surface was measured initially using a hand-held Hall probe positioned 0.5 mm from the surface. Prior to measurement the samples had been field cooled at 77 K in an applied magnetic field of 1.4 T. The temperature of the samples was maintained at 77 K for the duration of the measurements. In addition, the trapped field profile across both the top and bottom surface of each single grain was measured subsequently using a rotating array of 19 Hall probes positioned approximately 1.5 mm above the surface of each sample.

Measurement of the mechanical properties

The cutting and mechanical testing of the samples is described in [8].

Microstructural analysis

The remaining half of each sample used in the mechanical testing was polished and imaged using an optical microscope at 50× magnification. Images were taken throughout the cross-section to enable a detailed picture to be constructed from multiple images. In addition, images were taken at locations corresponding to the centre of the flexural beams. The use of Image J software [36] enabled quantification of the area fraction of each image occupied by pores and, where relevant, silver agglomerates. The colour threshold was adjusted to highlight the pores or silver agglomerates in a particular image and the 'analyse particles' tool was used to collect data on the area of the image occupied by these features.

Each of the flexural beams was also imaged after failure in order to study their fracture surfaces.

Results

Trapped field

Each of the 26 mm diameter samples exhibited a trapped field profile characteristic of a single grain sample, which consisted of a single peak with a smooth, continuously decreasing radial field gradient. An example of the trapped field profile for each of the three types of sample is shown in figure 1. The average maximum trapped field and the maximum variation in trapped field from sample to sample is shown in figure 2. The average maximum trapped field is very similar for all three sets of samples, as is the observed spread in maximum trapped field.

Mechanical properties

A three-point bend test was performed on 41 beams from each of YBCO and LR YBCO and 47 beams of YBCO-Ag. Seven beams from the YBCO-Ag samples and 13 beams from each of the LR YBCO and YBCO bulk samples contained large cracks or pores and did not survive the moving and cleaning process following cutting [8]. The average flexural strength of these beams can be found in [8]. There were only four locations where corresponding beams had noticeably higher strength than the YBCO-Ag beams. In addition, the highest overall flexural strength of 170 MPa was achieved in one of the YBCO-Ag beams. However, there was significant fluctuation in the flexural strength between beams from corresponding locations in different samples of nominally the same type and composition. This large fluctuation in mechanical strength is typical of brittle ceramics and is why the Weibull distribution is used regularly to characterise the strength of these materials [37].

In order to test whether the effect of adding silver or additional liquid phase on the flexural strength is statistically significant, a single factor analysis of variance (ANOVA) [38] was carried out on the data. ANOVA describes a group of statistical tests that are used to compare the variation both among and between groups of data. In this case, the mean values of the flexural strength of beams of YBCO, LR YBCO and YBCO-Ag have been compared. The value produced by ANOVA can then be compared to a critical value that takes into account the number of free variables both within each of the groups and between the groups. A range of statistical significance levels are defined subsequently, with the lower the number, the greater its significance. This analysis has shown that both the addition of silver and the provision of additional liquid phase does have a statistically significant effect on the flexural strength of beams of YBCO. The difference is statistically significant at the 5% significance level with $F_{crit}(2,122) = 3.0$ and $F = 12.8$, and therefore $F > F_{crit}$. This is itself, therefore, statistically significant.

We have shown that the flexural strength of YBCO can be increased significantly by the introduction of silver to the single grain microstructure. The provision of additional liquid phase alone improves the flexural strength of YBCO, but less so than the addition of silver.

Failure in brittle materials, such as the YBCO beams tested in this study, is due predominantly to cracks spreading from pre-existing flaws present within their microstructure. Therefore, the strength of these materials can be best represented as a distribution related to the probability of failure. The beam failure data can be used to derive the parameters for the Weibull distribution for the failure of YBCO, LR YBCO and YBCO-Ag beams under three-point bending. The

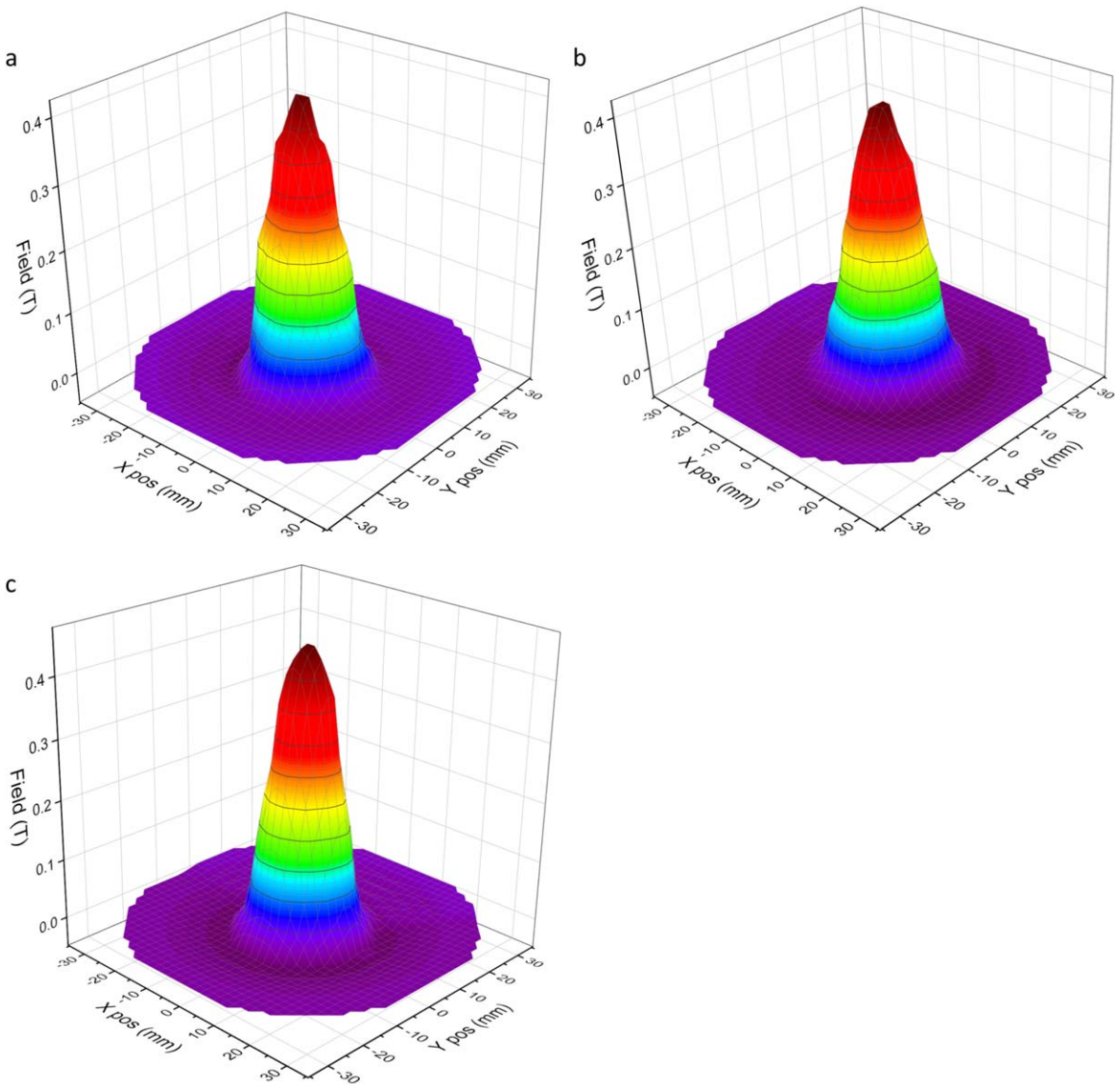

Figure 1. Trapped field profiles from single grains of: (a) YBCO, (b) LR YBCO and (c) YBCO-Ag.

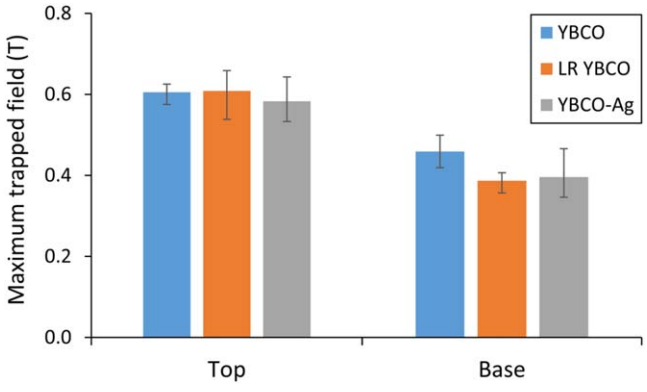

Figure 2. The average maximum trapped field recorded at the top and base of the samples.

Weibull distribution models for each system are given in table 1. The plots of the measured data and the predicted Weibull distributions are shown in figure 3. The R^2 values of the lines of best fit used to derive these parameters were 0.96, 0.91 and 0.98 for the YBCO-Ag, LR YBCO and YBCO systems, respectively. These values are reasonably high and so the best fit line is a relatively good fit to the data. Each sample and sub-specimen exhibits some variation and so this is likely to reduce the quality of the fit of the data to a particular model. However, the parent single grain bulk superconductors exhibit trends in the average pore and crack size at particular locations within the sample and so this may have an effect on the results observed for the flexural beams. It should be noted that all beams were assumed to be of identical size

Table 1. The Weibull distributions determined for the YBCO, LR YBCO and YBCO-Ag systems.

System	Weibull distribution
YBCO	$P_f = 1 - e^{-\left[\frac{\sigma}{37.7}\right]^{1.4}}$
LR YBCO	$P_f = 1 - e^{-\left[\frac{\sigma}{58.8}\right]^{2.5}}$
YBCO-Ag	$P_f = 1 - e^{-\left[\frac{\sigma}{67.0}\right]^{2.1}}$

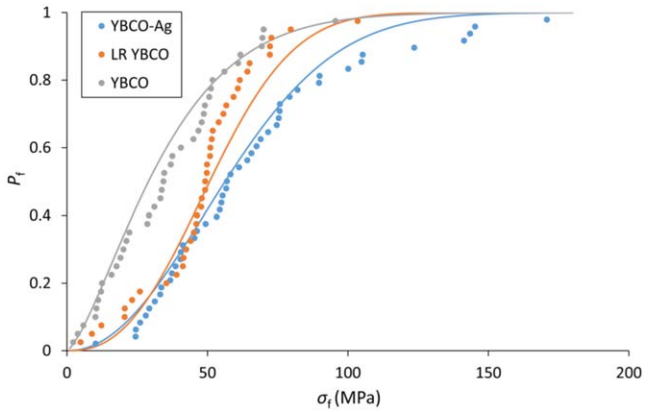

Figure 3. The predicted Weibull distributions (solid lines) compared with the measured data (dots).

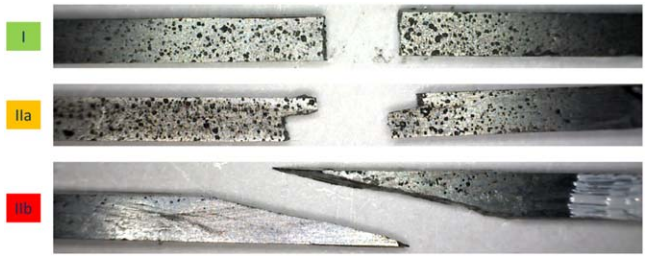

Figure 4. Examples of the three failure morphologies exhibited after the three-point bend test. The colours and letters correspond to labelling and colourings used in the later figures.

for the derivation of these parameters. This is true to a reasonable approximation.

The value of σ_o in the Weibull distribution is the stress level at which the sample has a probability of failure of 0.635. The YBCO-Ag system required the largest stress to yield this probability of failure, and is therefore stronger, on average, than LR YBCO, which, in turn, is stronger than YBCO (i.e. both LR YBCO and YBCO require an even lower stress to yield failure probability of 0.635). The parameter m represents the level of homogeneity, with larger values of m correlating with greater homogeneity in the flaw size and distribution and, hence, a smaller variation in flexural strength. The Weibull distributions suggest that YBCO has the lowest homogeneity of flaws, followed, in increasing homogeneity by YBCO-Ag and LR YBCO.

Fracture surfaces

The morphologies of the fracture surfaces produced after failure were studied, with examples shown in figure 4. The different break features are due to crack propagation along different crystallographic directions in the beam specimens. Type I failure exhibited a single facet and is due to stresses applied perpendicular to the fracture surface formed. Type II failure was classified into two forms; (a) those that exhibited multiple facets and (b) those that exhibited a single diagonal break. Type II failure is due predominantly to shear stresses acting parallel to the plane of the fracture surface formed and

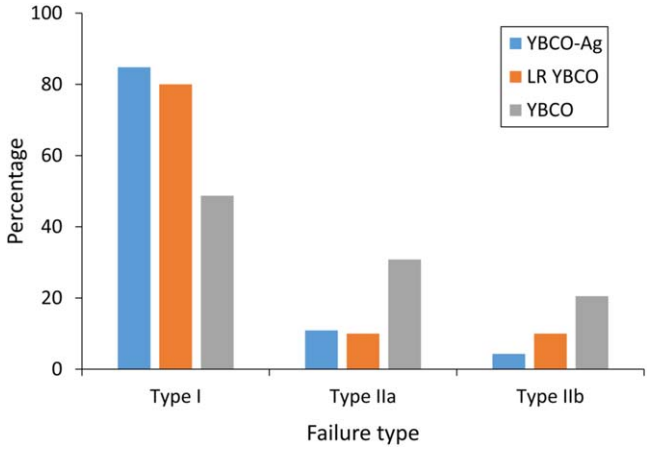

Figure 5. The percentages of beams that exhibited each type of failure morphology in each of the three systems.

is probably due to the effect of the cracks present on the distribution of stresses within the beam.

The percentages of each surface type produced in each type of sample after failure in the three-point bend tests are shown in figure 5. The YBCO-Ag and LR YBCO beams exhibited predominantly a Type I failure morphology with only 15% and 20% of the beams tested exhibiting one of the other two failure types observed for in YBCO-Ag and LR YBCO, respectively. However, in the YBCO system less than half of the beams exhibited a Type I surface failure morphology, with 31% and 21% exhibiting Type IIa and IIb failure, respectively. This suggests that the YBCO system contains more cracks oriented along the a/b-direction, and that these flaws facilitate delamination, leading directly to a Type II failure morphology in YBCO. In contrast, the additional liquid phase added to LR YBCO and the Ag added to YBCO-Ag help to reduce the occurrence and size of these a/b-direction cracks, and so these beams are more likely to exhibit a Type I failure morphology.

The failure morphology observed in each of the beams, including those that failed prior to 3-point bend testing, is shown schematically in figure 6. These plots show that the majority of Type IIb failures occurred in the YBCO beams and were observed generally near the centre of the sample. This is as expected, given that larger pores and cracks and a greater number of cracks are present at the centre of the sample. In addition, this shows that a large number of the samples that exhibited a Type IIb failure morphology were broken before testing.

The schematic plots shown in figure 6 have been compared with the ImageJ analysis of the area occupied by pores in the microscope image at the centre of the beam [8]. There is no obvious correlation between the total area occupied by pores and the failure morphology that occurred at the centre of the beam. In addition, single factor ANOVA has been performed to determine whether the difference in failure stress is significantly different between Type I, IIa and IIb failure modes. The difference is not statistically significant at the 5% significance level with $F_{crit}(2,124) = 3.1$ and $F = 2.0$, $F < F_{crit}$. Hence, the failure strength is not categorised by the

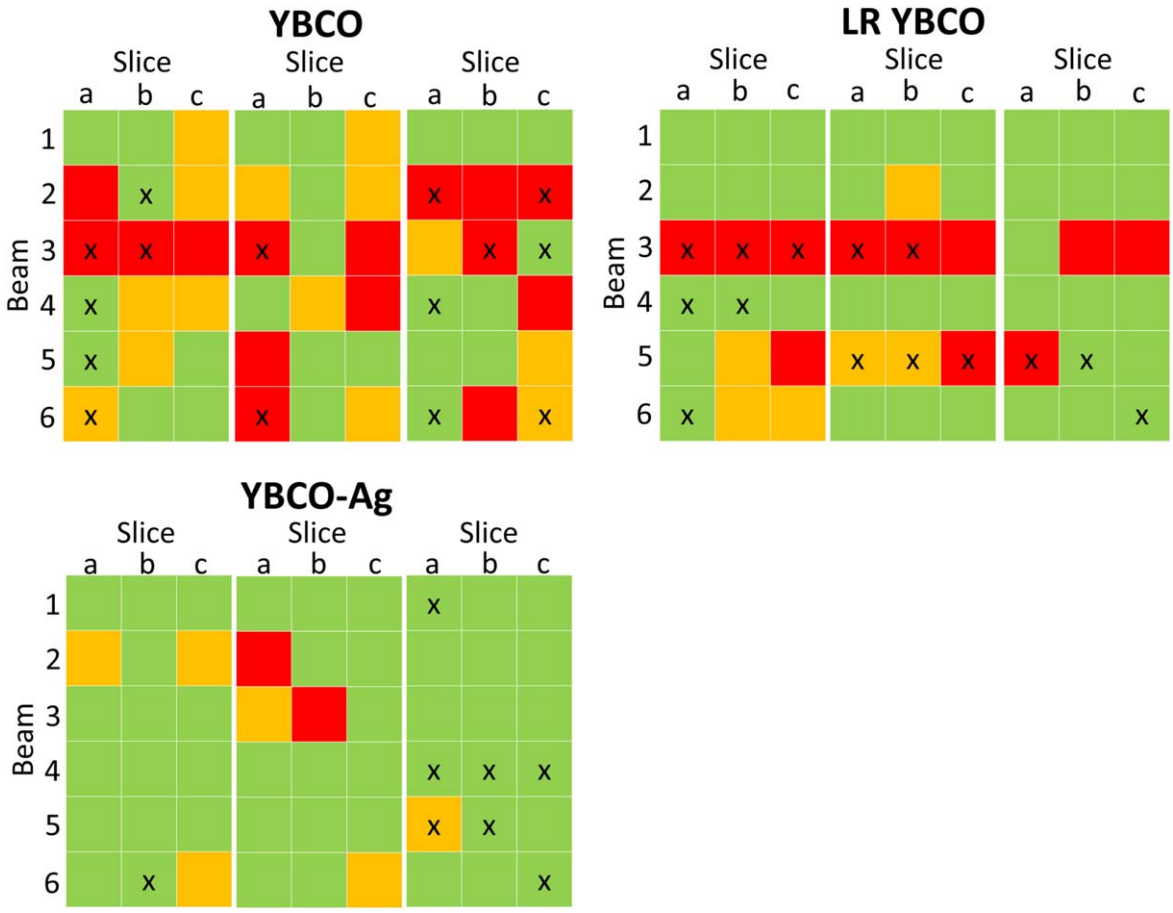

Figure 6. Schematic illustration of the failure surface type in each of the beams from each of the 9 samples tested using 3-point bending. Key: x—Failed before 3-point testing, Green—Type I, Yellow—Type IIa, Red—Type IIb.

type of failure surface produced. Although, the failure strength may be grouped by failure type within each of the YBCO, LR YBCO or YBCO-Ag groupings, there is insufficient data to test for statistical significance within each of the three material systems.

Figure 7 shows an example of the microstructure of the cross-section corresponding to slice a for one sample from each system. These whole images are built from smaller images taken at 50× magnification in order to illustrate the overall microstructure of the beams in slice a. The failure pattern of the beams from these cross-sections corresponds to slice a of the left-most sample of each type shown in figure 6. It can be seen that the YBCO sample contains a large number of relatively thick cracks (indicated by black lines in the images). The top of the sample is relatively free of large cracks and exhibited a Type I failure morphology. Both the pores (shown as black shapes in the figure) and cracks are larger and more noticeable closer to the centre of the sample (i.e. in the vertical direction). In this region the samples failed before testing, due almost certainly to the presence of large cracks. The large cracks clearly facilitated a Type IIb failure morphology.

The sample of LR YBCO exhibits some cracking but there are fewer large cracks present than in the YBCO sample. The top of the sample has a very limited number of cracks and a limited number of small pores and, as a result, the two beams at the top of the sample exhibited a Type I failure morphology. A large crack is present further down the sample, which corresponds to where the Type II failure morphology was observed in beam 3. The limited number and size of cracks and pores have reduced the number of locations at which a Type II failure mode occurs in the beams.

The YBCO-Ag sample exhibits fewer cracks and both smaller and fewer pores. There are also obvious silver agglomerates present (bright yellow in colour on the image) in the sample microstructure, and hence no Type IIb failure morphologies are observed in beams cut from this sample. The Type IIa failure morphology is likely to correspond to the large crack that can be seen at a position approximately $1/3$ from the top of the sample.

The cracking is thought to occur both due to the pressing and oxygenation processes. The addition of silver changes the composition of the powder, it becomes more ductile than the other precursor powders, and hence reduces the cracking and striations that occur during pressing. In addition, the silver inclusions may be able to reduce the stresses that typically cause YBCO bulk superconductors to crack during cooling in the TSMG process and during heating and cooling throughout oxygenation. The addition of silver is able to increase the flexural strength more than just the provision of additional

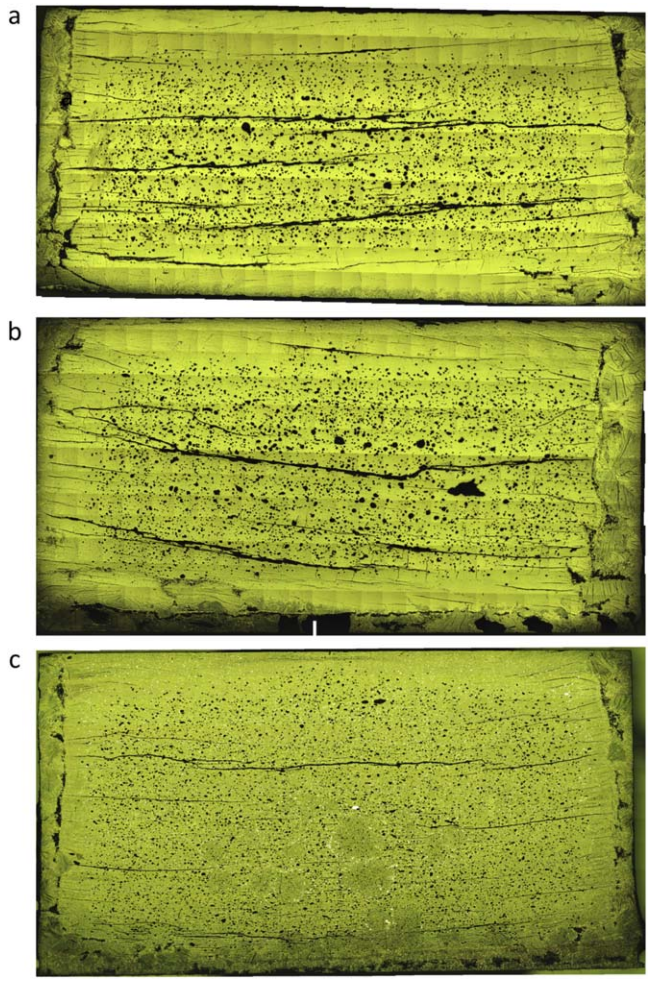

Figure 7. Images of the microstructure of the left-most single grain shown schematically in figure 6. (a) YBCO, (b) LR YBCO and (c) YBCO-Ag.

liquid phase despite LR YBCO having a greater homogeneity in the flaws present ($m = 2.5$ and 2.1 for LR YBCO and YBCO-Ag, respectively).

This work has demonstrated that the addition of silver to YBCO-Ag improves significantly the mechanical properties of YBCO, whilst maintaining a trapped field equivalent to that of YBCO. This study has also highlighted both the complexity of the process required to improve the mechanical strength and the variability in the mechanical properties within each single YBCO grain. The beams cut from the YBCO samples had the lowest flexural strength and these beams exhibited a greater number of Type II failure morphologies. This, when considered alongside the images of the sample microstructures, suggests, unsurprisingly, that large cracks are particularly detrimental to the mechanical strength of YBCO. Therefore, in order to improve the strength, we should try to reduce the likelihood of Type II failure shapes occurring and to do so should reduce the cracking and porosity present in the as-processed single grain. The provision of additional liquid phase and the addition of silver both appear to increase the strength of the YBCO beams. This is likely to be due to both the reduction in cracking and porosity and to the increase in the homogeneity and distribution of the flaws present within the samples.

In order to further improve the mechanical properties of YBCO the quantity of silver added could be optimised. In addition, the amount of additional liquid added could be optimised to further reduce the cracks and pores present. Alternatively, the heating profile could be modified to try to improve the homogeneity of the flaws present and enable more of the gas to diffuse out of the structure. Another way in which to reduce the likelihood of cracking is to add alternative alloying elements.

Although the mechanical properties are not better within the YBCO-Ag samples than in the YBCO samples at every location, this work has indicated that with further optimisation we should be able to achieve better mechanical properties throughout the YBCO-Ag samples. Therefore, further work is required to eliminate the weakest link, or indeed the most problematic flaw, present at each location within the YBCO bulk superconductor, and hence to improve the overall mechanical properties of the YBCO system, which is important for practical applications.

Conclusion

A detailed study of the failure of over 41 beams of each of YBCO, LR YBCO and YBCO-Ag single grain samples has been performed. However, as is generally the case for ceramic materials, the failure of these single grains is governed by critical flaws present in the sample microstructure and so the Weibull distribution was used to model the probability of failure. The so-called Weibull moduli, which measure sample homogeneity, for the YBCO, LR YBCO and YBCO-Ag systems had values of 1.4, 2.5 and 2.1, respectively, which are low for even that of a 'poor' ceramic, which lies typically between 1 and 10. This has illustrated that the homogeneity of flaws is more uniform in the LR YBCO and YBCO-Ag single grains than in YBCO.

The morphology of the failure surface exhibited by the three types of sample has been studied. This analysis suggests, unsurprisingly, that it is necessary to eliminate large crack critical flaws in order to improve the overall mechanical strength of YBCO. Typically, the width of the cracks found in the YBCO-Ag samples are sufficiently thin not to cause failure, whereas the crack thickness in the YBCO samples is sufficiently large to constitute a critical flaw.

We conclude, therefore, that any alloying additions or methods of processing that reduce the cracking and flaws present within the single grain YBCO microstructure will be beneficial to the mechanical properties of the sample. As a result, future work should focus on eliminating the weakest flaw or area containing the weakest flaws, which have been identified in this study to be large cracks formed during melt processing.

Acknowledgments

The authors would like to acknowledge the support of the Engineering and Physical Sciences Research Council (EPSRC grant ref. EP/P00962X/1) for financial support.

Additional data related to this publication is available at the University of Cambridge data repository [https://doi.org/10.17863/CAM.46040]. All other data accompanying this publication are directly available within the publication.

ORCID iDs

Jasmin V J Congreve https://orcid.org/0000-0002-2025-2155
Yunhua Shi https://orcid.org/0000-0003-4240-5543
Kai Yuan Huang https://orcid.org/0000-0001-7476-305X
John H Durrell https://orcid.org/0000-0003-0712-3102

References

[1] Campbell A M and Cardwell D A 1997 Bulk high temperature superconductors for magnet applications *Cryogenics* **37** 567–75
[2] Werfel F N *et al* 2012 Superconductor bearings, flywheels and transportation *Supercond. Sci. Technol.* **25**
[3] Li B Z, Zhou D F, Xu K, Hara S, Tsuzuki K, Miki M *et al* 2012 Materials process and applications of single grain (RE)-Ba-Cu-O bulk high-temperature superconductors *Physica* C **482** 50–7
[4] Nishio T, Itoh Y, Ogasawara F, Suganuma M, Yamada Y and Mizutani U 1989 Superconducting and mechanical-properties of YBCO-Ag composite superconductors *J. Mater. Sci.* **24** 3228–34
[5] Iida K, Babu N H, Shi Y H, Miyazaki T, Sakai N, Murakami M *et al* 2008 Single domain YBCO/Ag bulk superconductors fabricated by seeded infiltration and growth *8th European Conf. on Applied Superconductivity*. vol 97 ed S Hoste and M Ausloos (Bristol: Iop Publishing Ltd)
[6] Sakai N, Seo S J, Inoue K, Miyamoto T and Murakami M 2000 Mechanical properties of RE–Ba–Cu–O bulk superconductors *Physica* C **335** 107–11
[7] Konstantopoulou K, Shi Y H, Dennis A R, Durrell J H, Pastor J Y and Cardwell D A 2014 Mechanical characterization of GdBCO/Ag and YBCO single grains fabricated by top-seeded melt growth at 77 and 300K *Supercond. Sci. Technol.* **27** 11
[8] Congreve J V J, Shi Y H, Huang K Y, Dennis A R, Durrell J H and Cardwell D A 2019 Improving mechanical strength of YBCO bulk superconductors by addition of Ag *IEEE Trans. Appl. Supercond.* **29** 5
[9] Cook R F, Dinger T R and Clarke D R 1987 Fracture-toughness measurements of $YBA_2CU_3O_X$ single-crystals *Appl. Phys. Lett.* **51** 454–6
[10] Raynes A S, Freiman S W, Gayle F W and Kaiser D L 1991 Fracture-toughness of $YBA_2CU_3O_6$+delta single-crystals—anisotropy and twinning effects *J. Appl. Phys.* **70** 5254–7
[11] Ochiai S, Osamura K and Takayama T 1988 Fracture-toughness measurements of $BA_2YCU_3O_{7-X}$ superconducting oxide by means of indentation technique *Japan. J. Appl. Phys.* 2 **27** L1101–3
[12] Goyal A, Oliver W C, Funkenbusch P D, Kroeger D M and Burns S J 1991 Mechanical properties of highly aligned $YBa_2Cu_3O_7-\delta$ effect of Y_2BaCuO_x particles *Physica* C **183** 221–33
[13] Okudera T *et al* 2003 Fracture toughness evaluation of YBCO bulk superconductor *Physica* C **392–396** 628–33
[14] Goyal A, Funkenbusch P D, Kroeger D M and Burns S J 1991 Fabrication of highly aligned $YBa_2Cu_3O_7-\delta$-Ag melt-textured composites *Physica* C **182** 203–18
[15] Fujimoto H, Murakami M and Koshizuka N 1992 Effect of Y_2BaCuO_5 on fracture toughness of YBCO prepared by a MPMG process *Physica* C **203** 103–10
[16] Konstantopoulou K, Roa J J, Jimenez-Pique E, Segarra M and Pastor J Y 2014 Fracture micromechanisms and mechanical behavior of YBCO bulk superconductors at 77 and 300 K *Ceram. Int.* **40** 12797–806
[17] Huang K Y *et al* 2018 Spatial distribution of flexural strength in Y–Ba–Cu–O bulk superconductors *IEEE Trans. Appl. Supercond.* **28**
[18] Fujimoto H 2003 Flexural strength of melt-processed Y–Ba–Cu–O bulk superconductors with Ag addition measured at 77 K *Supercond. Sci. Technol.* **16** 1115–9
[19] Hondros G 1959 The evaluation of Poisson's ratio and the modulus of materials of low tensile resistance by the Brazilian (Indirect tensile) test with particular reference to concrete *Australian J. Appl. Sci.* **10** 243–68
[20] Murakami A *et al* 2002 Tensile strength and fracture surface topography of Sm–Ba–Cu–O bulk superconductors *Supercond. Sci. Technol.* **15** 1099–104
[21] Dimos D, Chaudhari P, Mannhart J and Legoues F K 1988 Orientation dependence of grain-boundary critical currents in $YBa_2Cu_3O_7$-delta bicrystals *Phys. Rev. Lett.* **61** 219–22
[22] Todt V R, Zhang X F, Miller D J, StLouisWeber M and Dravid V P 1996 Controlled growth of bulk bicrystals and the investigation of microstructure-property relations of $YBa_2Cu_3O_x$ grain boundaries *Appl. Phys. Lett.* **69** 3746–8
[23] Durrell J H, Hogg M J, Kahlmann F, Barber Z H, Blamire M G and Evetts J E 2003 Critical current of $YBa_2Cu_3O_7$-delta low-angle grain boundaries *Phys. Rev. Lett.* **90**
[24] Cardwell D A 1998 Processing and properties of large grain (RE)BCO *Mater. Sci. Eng.* B **53** 1–10
[25] Shiohara Y and Endo A 1997 Crystal growth of bulk high-T-c superconducting oxide materials *Mater. Sci. Eng.* R **19** 1–86
[26] Nariki S, Sakai N, Murakami M and Hirabayashi I 2004 High critical current density in RE–Ba–Cu–O bulk superconductors with very fine RE_2BaCuO_5 particles *Physica* C **412** 557–65
[27] Murakami M, Yamaguchi K, Fujimoto H, Nakamura N, Taguchi T, Koshizuka N *et al* 1992 Flux pinning by nonsuperconducting inclusions in melt-processed YBaCuO superconductors *Cryogenics* **32** 930–5
[28] Sakai N, Seo S-J, Inoue K, Miyamoto T and Murakami M 1999 Cracking mechanisms and tensile strengths for melt-processed RE–Ba–Cu–O (RE: Sm, Y) *Advances in Superconductivity XI* (Tokyo: Springer) pp 685–8
[29] Congreve J V J, Shi Y H, Dennis A R, Durrell J H and Cardwell D A 2018 The successful incorporation of Ag into single grain, Y–Ba–Cu–O bulk superconductors *Supercond. Sci. Technol.* **31** 7
[30] Congreve J V J, Shi Y H, Dennis A R, Durrell J H and Cardwell D A 2019 Comparison of the superconducting properties of Y–Ba–Cu–O and Y–Ba–Cu–O–Ag bulk superconductors *IOP Conf. Ser.: Mater. Sci. Eng.* **502** 012181
[31] Griffith A A 1968 Phenomena of rupture and flow in solids *Asm Trans. Q.* **61** 871
[32] Jayatilaka A D S and Trustrum K 1977 Statistical approach to brittle fracture *J. Mater. Sci.* **12** 1426–30

[33] Trustrum K and Jayatilaka A D S 1979 On estimating the Weibull modulus for a brittle material *J. Mater. Sci.* **14** 1080–4

[34] Congreve J V J, Shi Y H, Dennis A R, Durrell J H and Cardwell D A 2017 Improvements in the processing of large grain, bulk Y–Ba–Cu–O superconductors via the use of additional liquid phase *Supercond. Sci. Technol.* **30** 11

[35] Congreve, Y J V J S, Dennis A R, Durrell J H and Cardwell D A 2017 The successful incorporation of Ag into single grain, Y–Ba–Cu–O bulk superconductors *IOP Conf. Ser.: Mater. Sci. Eng.*

[36] Schneider C A, Rasband W S and Eliceiri K W 2012 NIH Image to ImageJ: 25 years of image analysis *Nat. Methods* **9** 671

[37] Weibull W 1951 A statistical distribution function of wide applicability *J. Appl. Mech.-Trans. ASME* **18** 293–7

[38] Fisher R A 2009 Studies in crop variation. I. An examination of the yield of dressed grain from Broadbalk *J. Agric.Sci.* **11** 107–35